Effects of Exhausts from Aluminized Solid Propellants on Launch Facilities

EDWARD J. LAYS* AND EUGENE A. DARROW†
Martin Marietta Corporation, Denver, Colo.

The effects of solid propellant rocket motor (SRM) aluminum content, chamber pressure, nozzle exit diameter, and lift-off acceleration have been evaluated with respect to degradation of protective coatings applied to flame deflectors and umbilical masts. After investigation of the properties and characteristics of commercially available protective coatings, several of the most promising materials were evaluated in detail during scale-model firings, and design nomographs for these materials are illustrated. These data and the scaling factors have been correlated with full-scale effects data compiled from launch histories of Titan IIIC. The investigation revealed that deflector erosion was not proportional to aluminum content of the propellant, and that erosion was influenced to a great extent by the manner in which the aluminum affected the burning characteristics (chamber temperature) of the propellant. The thermal energy of the exhaust plume, rather than the abrasive quality of aluminum particles, was the major source for erosion. Erosion was roughly proportional to the motor chamber pressure squared, and varied inversely with the square root of lift-off acceleration when lift-off acceleration was expressed in nozzle diam/sec².

Nomenclature

A = area
D_e = nozzle exit diameter
h = heat-transfer coefficient
I_{sp} = specific impulse
p_c = chamber pressure
q = quantity of heat per unit time
Q = quantity of heat
r = radial distance from nozzle centerline
t_b = burn time
$\dot{w}$ = weight flow rate
x = axial distance aft of nozzle exit, or distance along deflector surface as measured from centerline of impingement, positive downstream
ϵ = nozzle expansion ratio

Introduction

LARGE SRM's are being considered for a variety of applications involving augmented and improved Saturn launch vehicles. In evaluating existing facilities for applicability and the modifications needed to accommodate the many proposed configurations, it became apparent that little was known about the effects of SRM exhaust on flame deflectors, launch duct walls, launchers, umbilical masts, and umbilical towers. Liquid rocket motor technology was not applicable because of the absence of aluminum particles commonly used in SRM grains. Applicable captive firing data are completely lacking, because SRM's are tested in such an attitude that they exhaust directly into the atmosphere, thereby minimizing complicated facility requirements. Recognizing this deficiency, NASA contracted with Martin Marietta Corporation, Denver division, for the solid propellant rocket exhaust effects (SPREE) program described in this paper.

Phase 1 of the SPREE program consisted of the gathering and evaluation of data from industry and government sources pertaining to SRM performance parameters, exhaust characteristics and environments, and commercially available insulator and ablator protective materials. These data were used to develop mathematical prediction models for defining the launch environment and its effects, and to plan an experimental program to verify the predication models. Phase 2 involved the validation and improvement of the prediction models and associated theories via test and included the correlation of model and full-scale data. Specific phase 2 objectives were to: 1) define the pressure and thermodynamic environment created by contemporary SRM's; 2) develop an understanding of the mechanism of erosion as it relates to aluminized SRM's; 3) evaluate and select deflector coating materials that provide adequate deflector protection and are economical to apply, maintain, and refurbish; 4) evaluate and select materials that will economically protect launch site structures from exhaust plume products; 5) determine the effect of SRM aluminum content, chamber pressure, nozzle size and cant, and lift-off acceleration on the erosion of flame deflectors and surfaces nearly parallel with the exhaust flow; and 6) determine the effect of repeat firings on deflector erosion.

Submitted November 17, 1966; revision received February 17, 1967; also presented as Paper 66-972 at the AIAA Third Annual Meeting, Boston, Mass., November 29–December 2, 1966. Work performed under Contract NAS10-2300 for NASA John F. Kennedy Space Center. [4.06, 10.05]

* Staff Engineer, Propulsion Research.
† Program Manager, Advanced Ground Systems. Member AIAA.

Theoretical Considerations

Types of Erosion

Two energy sources in SRM exhaust produce erosion: the kinetic and thermal energies of the gas and alumina particles. If the exhaust were cool, erosion would result solely from the kinetic energy source, with the solid particles contributing substantially. Exhaust products hot enough to melt a coating will produce erosion primarily as a result of thermal effects. Virtually all deflector and ground support equipment (GSE) coating materials melt or sublime when exposed directly and at close range to the exhaust products from present SRM's. Most erosion occurs during the short interval after ignition when the launch vehicle is moving slowly and is close to the surface on which it impinges. During the phase 1 SPREE effort, it was postulated that deflector erosion in a launch environment characteristic of the improved Saturn class of vehicles would be predominantly (90%) due to thermal effects. Confirmation of this supposition was sought during subsequent testing.

Scale Effects

It was suggested that if small motor lift-off acceleration were equal to that of a larger motor when acceleration is expressed in nozzle diam/sec², the depth of erosion produced by both motors should be nearly equal. Critics of this sug-

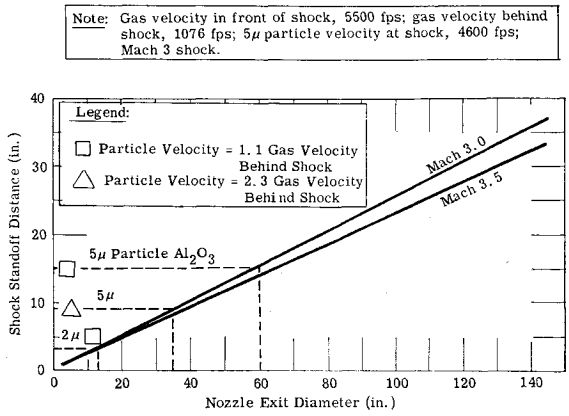

Fig. 1 Effect of scale on particle velocity during flat-plate impingement.

gestion said that the relationship would be in error for streams containing solid particles, because the shock waves produced by a large rocket motor would stand off from the surface being impinged on a greater distance than would the shock waves produced by a smaller motor (Fig. 1). The particles in the stream behind the larger motor would have more time to decelerate in the more extensive adverse pressure field behind the shock than would particles from the smaller motor. Therefore, large SRM's would produce less erosion. Others thought that the erosion profile produced by a small motor would be more concave than that produced by a large

Table 1 Propellant formulations

	Content (%)			
Aluminum	7.0	14.0	18.0	22.0
Polybutadiene acrylic acid	19.8	17.3	16.5	15.7
Ammonium perchlorate	69.0	65.0	62.0	59.0
ERL-2795 epoxy resin	4.2	3.7	3.5	3.3

motor because of an erosion depth similarity and the much smaller footprint. The concavity would produce a greater exhaust gas turning, leading to increased erosion.

Confirmation of the erosion scaling hypothesis was sought during SPREE testing. The method involved the scale-model simulation of the Titan IIIC United Technology Corporation (UTC) 120-in. SRM's launched from Eastern Test Range (ETR) Complex 40, and the obtaining of model- and full-scale erosion data for comparison.

Test Program

Scale-model testing was divided into three groups to allow maximum use of results from a group of firings before committing to the next. The first tests used cold-jet streams and were aimed at deriving critical relationships between the exhaust plume and deflector orientations and geometry.

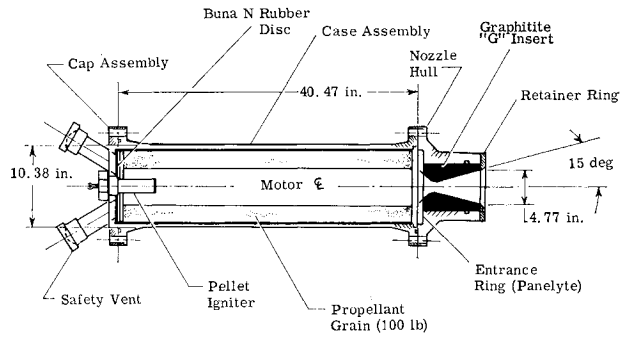

Fig. 2 13-sec rocket motor schematic.

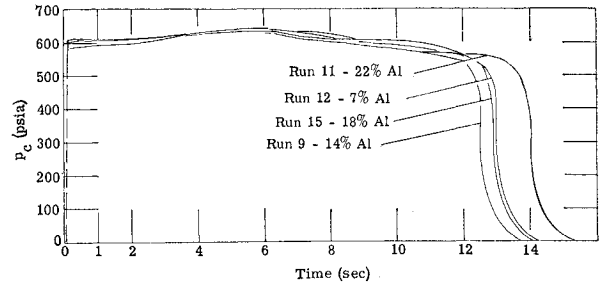

Fig. 3 Chamber pressure overlay for motors with varying percentages of aluminum.

The second group of tests consisted of 27 firings of small SRM's to verify the theoretical evaluations generated previously and to validate predictions of key SRM influencing factors. The third group of tests consisted of 27 hot firing runs to validate prediction models. Even during this final group of firings, deviations from the planned run schedule were made to allow adjustment of firings to meet outstanding requirements as they developed during the program.

Two types of SRM's were designed and fabricated: a 24-sec burn-time motor for firings simulating low lift-off thrust-to-weight ratios and a 13-sec burner. Both motor types were designed to produce approximately 2200 lb of thrust at similar chamber pressures and mass flow rates. Figure 2 shows the 13-sec motor design. The basic grain configuration was cylindrical with a center perforation and open ends; one end was slotted. The grains were cast in a paper phenolic case by the standard mandrel casting cure process. Propellant formulations are shown in Table 1. Motor performance was excellent in regard to the neutrality and reproducibility of chamber pressure (Fig. 3).

The test environment was produced by firing SRM's on test articles mounted on a mobile cart, which was allowed to move away from the SRM's at preprogrammed rates. This was accomplished with the acceleration control mechanism shown in Fig. 4. It was operated by a constant-speed, 40-hp electric motor that drove two gear reduction boxes interconnected by drive chains to a large swing arm. The swing arm paid out cable to the test cart at a rate consistent with the desired programmed acceleration. Varying rates of acceleration were achieved by interchanging gears in combination with varying the swing arm radius. The SRM was ignited by the swing arm as it traveled through its operational cycle. A gravity-drive mechanism was provided to insure a continuous pull on the test cart, so that positive nonlagging movement was insured during the full range of test accelerations. Accelerations within 5% of preprogrammed values were consistently achieved.

Figure 5 shows the test cart with the deflector and simulated umbilical tower and instrumentation. The small test panels coated with preselected protective coatings and the deflector

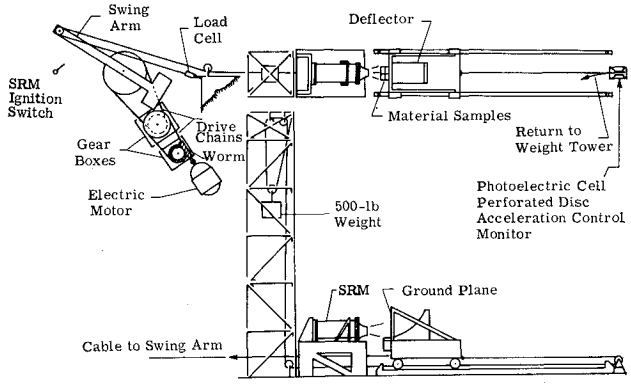

Fig. 4 Acceleration control test fixture.

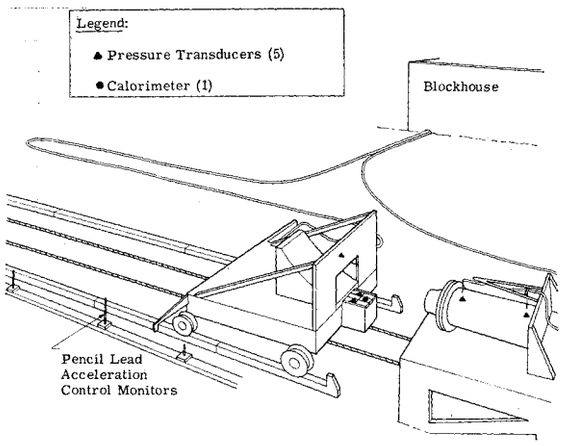

Fig. 5 Test instrumentation.

were carefully measured and weighed before and after each firing. To obtain exhaust plume measurements, a graphite-coated steel rake was installed on the stripped-down cart, which then was allowed to travel down the track (beginning at eight nozzle diameters downstream of the motor) away from the SRM.

Environments Created by Exhaust

Environment data were obtained during the SPREE program and during full-scale firings of UTC 120-in. SRM's. SPREE plume data were obtained for the 7% aluminum

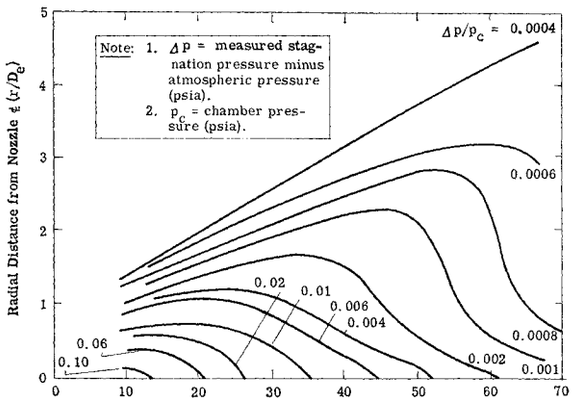

Fig. 6 Exhaust plume stagnation pressure and temperature profiles.

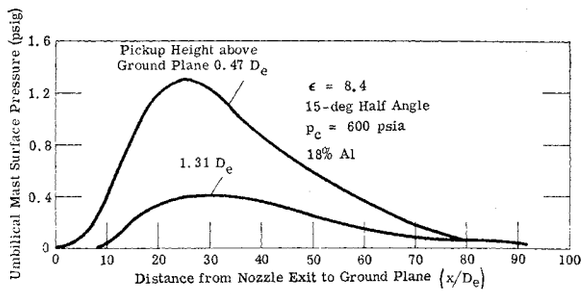

Fig. 7 Variation of umbilical mast surface pressure during lift-off (lateral offset, 1.5 D_e).

propellant. (Measurement problems were encountered when grains with higher aluminum percentages were used.) Because of the relatively low Al content, the severity of the exhaust environment was somewhat less than that for contemporary solids, and allowances are required when using the data. Figure 6 shows the results of a single plume traversing probe. Surface pressures on an umbilical mast situated a constant 1.5 nozzle exit diameter (D_e) laterally from a plume centerline are shown in Fig. 7 as a function of lift-off distance.

The rate at which heat was delivered to an asymptotic calorimeter situated on a vertical surface 1.5 D_e from an SRM exhaust plume centerline during a simulated lift-off is shown in Fig. 8. Umbilical mast heating rate data similarly obtained during a full-scale Titan IIIC launch also are shown. The heating rates shown would, of course, be higher if the missile were to drift toward the surface during launch.

Thermal radiation data were obtained during two static firings of UTC 120-in. SRM's exhausting vertically upward. One firing was made with Thrust Vector Control (TVC) injection and the other without it. Average radiation flux values obtained are listed in Table 2. The maximum measured radiation fluxes for the firing without TVC injection are also listed. Note that the N_2O_4 injectant reduces the radiation levels. Apparent plume emissive power data derived from information in Table 2 and in Refs. 1 and 2 are shown in Fig. 9.

Near-field acoustic spectra obtained at four discrete times during a Titan IIIC launch are shown in Fig. 10. The data were obtained via a microphone located at the top of the umbilical tower approximately 31 ft (3.5 D_e) from each UTC 120-in. SRM.

Deflector Coating Materials

Some of the properties considered in the selection and ultimate evaluation of a deflector coating were: resistance to thermal shock, strength at high temperature, length change at very high temperature, spall resistance, resistance to crack propagation, resistance to acoustic shock, insulation properties (steel reinforcement when heated will expand and might crack the coating), ability to be applied by the Gunite process, and ability to be cured by normal procedures without cracking.

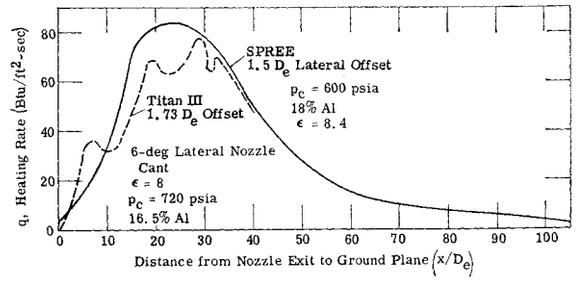

Fig. 8 Umbilical mast heating environment during lift-off.

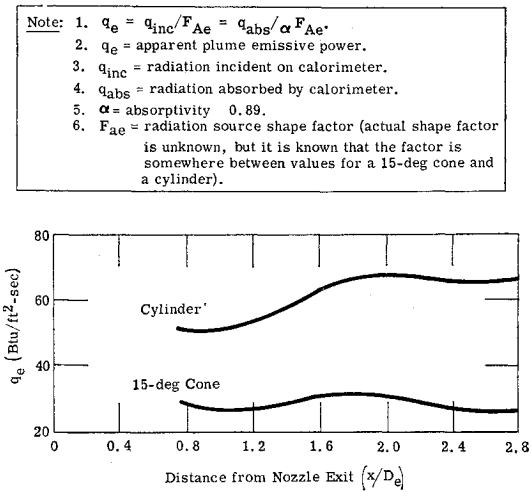

Fig. 9 UTC 120-in. SRM apparent plume emissive power.

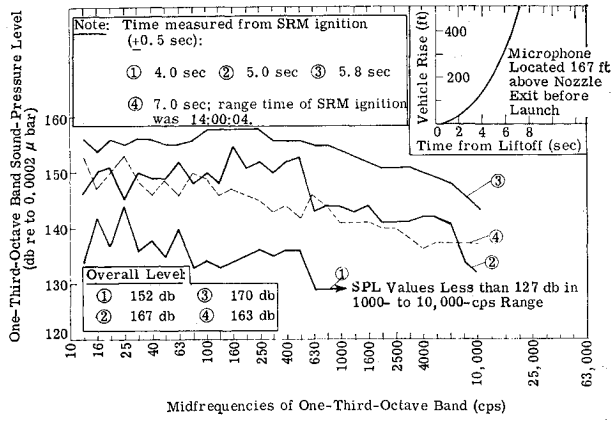

Fig. 10 Correlation of Titan IIIC acoustic spectra with time.

All coatings considered had good insulation properties and could be applied by the Gunite process. The five candidates chosen for evaluation were: Fondu Fyre WA-1 and XB-1 (Pryor Giggey Company, Whittier, Calif.); H-W Harcast ES and Special Mix 13-65 Fused Silica Castable (Harbison-Walker, Fulton, Mo.); and Portland cement (reference material).

All coatings except H-W Harcast ES and Portland cement were designed specifically for flame deflectors. Harcast ES was developed for extreme abrasion applications and has been used for petroleum refinery equipment, cyclones, and piping. Fondu Fyre WA-1 is a premixed combination of selected refractory aggregates and a hydraulic setting binder. It has a high Al_2O_3 and Fe_2O_3 content. (Fe_2O_3 is a good infrared emitter.) Fondu Fyre XB-1 has a high ZrO_2 content. H-W Harcast ES is a refractory castable consisting of calcined grog blended with calcium aluminate binder. H-W Special Mix 13-65 is a blended mixture of fused silica aggregate and a calcium aluminate hydraulic setting cement. Portland cement has a high CaO content.

Relative Performance

The relative performances of Fondu Fyre WA-1, Fondu Fyre XB-1, and Portland cement mixes under static firing conditions are shown in Fig. 11. The static firings were made with the SRM's 3 D_e from flat-plate deflectors. The deflectors were oriented at a 30° angle with respect to the flame centerline. Centerline erosion profiles are shown. The Fondu Fyre XB-1 eroded the least, followed by Fondu Fyre WA-1 and the Portland cement mix. The XB-1 spalled badly, however, as did the Portland cement, and extra care was required in curing the XB-1. The initial XB-1 pour cracked when burlap sacks used for curing dried out prematurely. No cracking problem was encountered with the Portland cement and WA-1 deflectors under similar curing conditions.

The relative performance of Fondu Fyre WA-1 and H-W Special Mix 13-65 under simulated lift-off conditions is shown in Fig. 12a. The H-W material eroded less than the WA-1, but it spalled badly. The WA-1 was superior to Harcast ES from an erosion depth standpoint. The WA-1 had no spalling tendency, it could be refurbished easily, and a built-in crack for one test showed no tendency to propagate. Because of its many fine attributes and relatively low cost, Fondu Fyre WA-1 was chosen as the best all-round deflector coating material.

Table 2 Radiation (Btu/ft²-sec) from UTC 120-in. SRM[a]

Sensor, x/D_e	Without TVC injection q_{max}	Without TVC injection q_{av}	With TVC injection q_{av}
2.83	11.1	10.7	9.3
2.38	10.8	10.4	8.8
1.93	11.3	10.8	8.6
1.47	10.1	9.6	8.4
1.02	9.2	8.1	7.5
0.79	8.5	8.1	7.3
0.79[b]	1.7	1.0	0.6

[a] All calorimeters 1.8 D_e from motor centerline laterally. Nozzle is canted 6° away.
[b] Shielded calorimeter.

Behavior Prediction

The effect of SRM aluminum content, chamber pressure, scale, nozzle cant, and lift-off acceleration on deflector erosion under simulated lift-off conditions was determined using Fondu Fyre WA-1 J deflectors. The point of initial impingement was 3 D_e from the SRM nozzle exit, and the flame centerline made an angle of 30° with the J.

Figure 12b shows the effect of propellant Al content. Maximum erosion occurred when the grain containing 18% Al was used. Progressively less erosion resulted from firings with the 14, 22, and 7% grains with no apparent relation to % Al. Additionally, there was no apparent relation between erosion and propellant I_{sp} values as determined from standard Rohm and Haas firing tests.‡

Early SPREE Tests[3] were made to evaluate the effect of SRM chamber pressure (p_c) on erosion. The tests were made with SRM's having nominal p_c of 700 and 1100 psia.

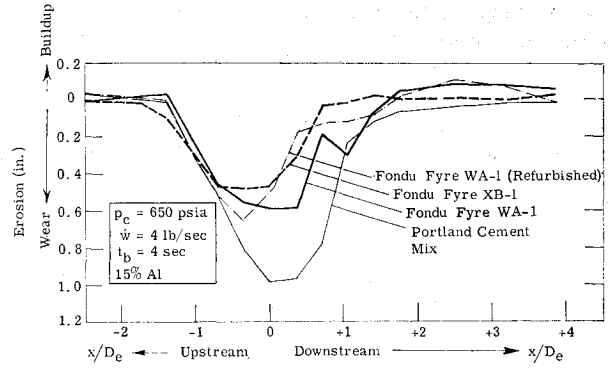

Fig. 11 Erosion resistance of Fondu Fyre and Portland cement mixes on deflector centerline.

‡ Propellant I_{sp} values with a nonoptimized nozzle, as determined by Rocket Power Inc. for 7, 14, 18, and 22% Al, were 224, 234, 222, and 196 sec, respectively.

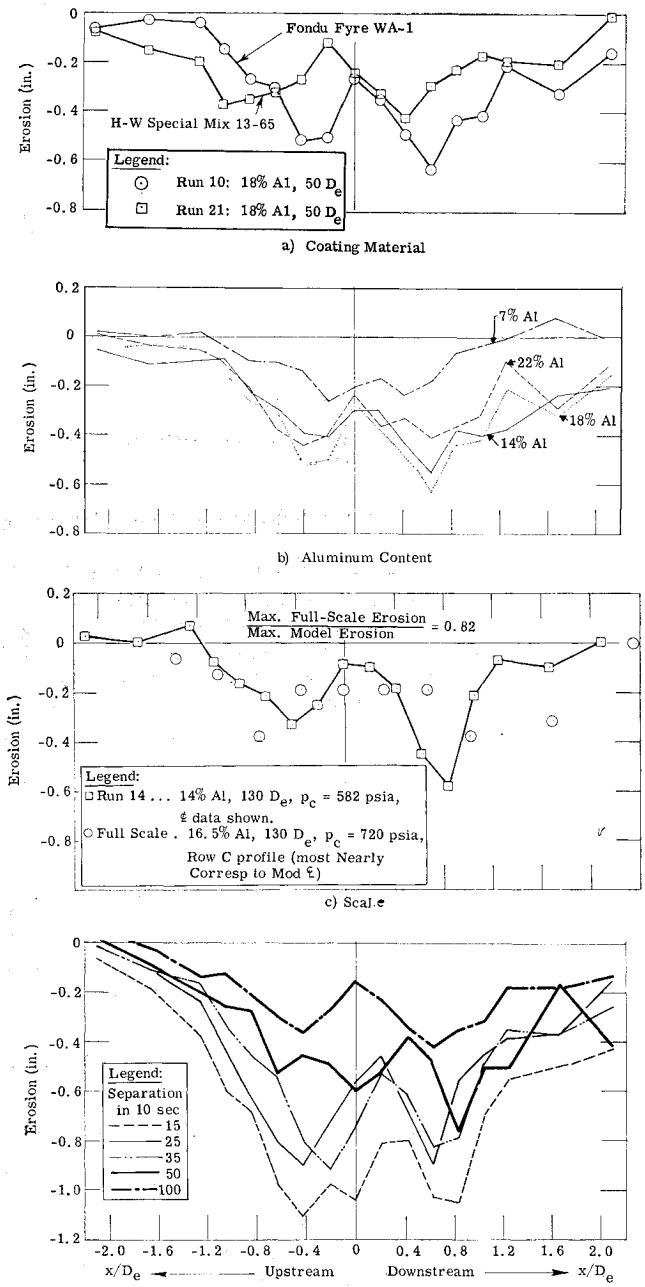

Fig. 12 Effects of coating material, aluminum content of propellant, motor scale, and lift-off acceleration on deflector centerline erosion.

The limited data obtained during these tests, although not conclusive, suggested that erosion was proportional to p_c^2. This finding was entirely unsuspected and could not be confirmed by theoretical considerations. Nevertheless, the relationship was adopted to provide a conservative means for erosion prediction.

Scale effects were investigated using a model deflector similar to the full-scale Titan IIIC flame deflector, coated with a Portland cement mix formulated in a manner similar to that for the full-scale counterpart. The aggregate was crushed and screened per specifications for the Complex 40 and 41 deflectors, and cement/aggregate proportions were duplicated. The model deflector was cast, but the full-scale deflector was coated by the Gunite process. Coatings applied by high-pressure gunning are denser and stronger than cast coatings. The model SRM was positioned with a 6° nozzle cant to simulate the UTC 120-in. nozzle

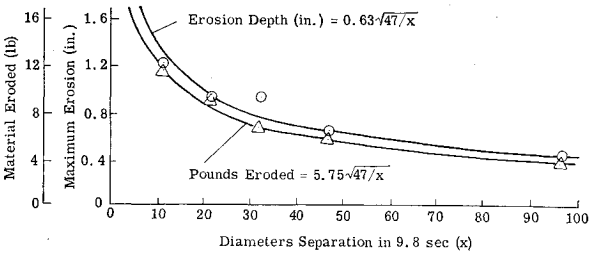

Fig. 13 Effect of lift-off acceleration on erosion.

cant. Lift-off was simulated by duplicating the full-scale lift-off acceleration expressed in nozzle diam/sec². Model- and full-scale erosion was measured at more than 70 points. Figure 12c shows the centerline erosion profiles. The greater maximum model erosion could be due to the less dense deflector coating, the reduced shock standoff distance, and/or the greater concavity of the eroded surface. Agreement is good in view of the vast scale difference. These tests confirmed the applicability of matching lift-off acceleration by the diam/sec² relationship. This relationship, when used for full-scale erosion predictions, produces slightly conservative results.

Tests to evaluate the effect of a 6° nozzle cant revealed that erosion is reduced 8 to 33% because of cant. The variation is due to thrust buildup characteristics and the type of deflector coating involved.

The important effect of lift-off acceleration on erosion is shown in Fig. 12d, which shows erosion profiles for various separations x/D_e attained 10 sec after SRM ignition (hold-down = 0.2 sec, and initial separation = 3 D_e). The information obtained at the several lift-off accelerations was used to develop a technique for predicting the erosion at any desired acceleration, given erosion data for any other lift-off acceleration. It was also used to determine whether there was a correlation with heat environment data.

Maximum erosion depth and deflector weight loss information are shown in Fig. 13 for several lift-off accelerations. The curves through the data show that erosion is inversely proportional to the square root of the separation attained in 9.8 sec. The values 0.63 and 5.75 in the figure represent the maximum erosion depth and maximum weight loss of a small-scale deflector as a result of an SRM lifting off so as to separate 47 D_e in 9.8 sec.

Heat-transfer coefficient h, as it relates to the SRM exhaust gas environment, is proportional to $(p_t\ U/T_t)^{0.8}$, where p_t = stagnation pressure, U = axial velocity, and T_t = stagnation temperature of exhaust plume gases. The plume profile

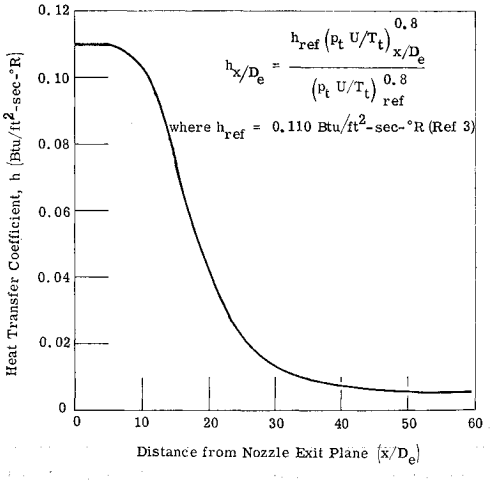

Fig. 14 Variation of exhaust plume centerline heat-transfer coefficient with distance from nozzle exit.

used to determine h values was assembled from rake pressure and temperature data, and velocity data from a 120-in. SRM. The reference h, 0.11 Btu/ft²-sec-°R, was assumed constant from the nozzle exit plane to a point 5 D_e downstream from the exit plane; h values aft of this point were then computed from plume profile and reference h data (Fig. 14). Plume centerline heat-transfer rates were computed for various downstream positions assuming a 1000°F impingement surface temperature. Total incident heat per unit area Q/A was obtained by graphically integrating qdt/A for the appropriate acceleration history. Table 3 shows the correlations of total heat ratio with deflector weight loss and maximum erosion depth ratios. The basis of the correlation is data from the test at the 47D_e-in. 9.8-sec lift-off acceleration (50 D_e separation attained at 10 sec). The good correlation indicates that erosion is predominantly due to thermal effects.

A repeat firing on a Fondu Fyre WA-1 deflector showed that erosion during a second firing was 1.36 to 1.38 times that of the first firing. However, because of the geometric dissimilarity between the model- and full-scale erosion profiles, the full-scale second-firing erosion should be smaller (see scale effects discussion).

The nomograph in Fig. 15 allows prediction of deflector erosion depth as a function of materials used, lift-off acceleration, and several SRM characteristics. These data conservatively predict the erosion for the first exhaust exposure. A second exposure yields up to 1.38 times the erosive effects of the first.

Coating Materials for Near-Parallel Flow Regime

There are launch situations during which ground winds cause the missile to drift close to structures and immerse them well within the exhaust plume. Without some kind of thermal protection, thermal stresses, buckling, and perhaps even structural failures would occur. SPREE work indicated that if a steel structure in near-parallel flow remained at least 1.5 D_e laterally from the centerline of an SRM exhaust plume, it would probably not be damaged by thermal effects during launch, provided the booster separated at least 50 D_e from the pad in 10 sec. This separation rate corresponds to a lift-off thrust-to-weight ratio of 1.25 for a 100-in. nozzle, 1.50 for a 200-in. nozzle, etc. At lower lift-off rates or where drift brings the booster closer than 1.5 D_e to the steel structure, some type of thermal protection is in order.

A low-density coating is especially desirable for structures on large mobile launchers which already are difficult to move. Protective coatings should be viscous and set rapidly so as not to sag when applied to vertical surfaces. They should be easy to apply, adhere firmly, and have a high resistance to thermal and acoustic shock as well as the high-temperature erosive environment of an aluminized SRM, and they must not burn after the booster leaves the pad. Compatibility with exhaust residue from the booster and any liquid propellants that might be used is another requirement. These chemicals should not react hypergolically with the coating or cause it to deteriorate. The coating should weather well, and it should be semi-elastic, easy to refurbish locally, and inexpensive.

Table 3 Correlations of weight loss and erosion depth with heat load

x/D_e attained at 10 sec	Heat load, Q/Q_{ref}	Weight loss, $\Delta W/\Delta W_{ref}$	Erosion depth, d/d_{ref}
15	1.91	2.00	1.92
25	1.45	1.56	1.48
35	1.18	1.19	1.48
50	1.00	1.00	1.00
100	0.71	0.70	0.70

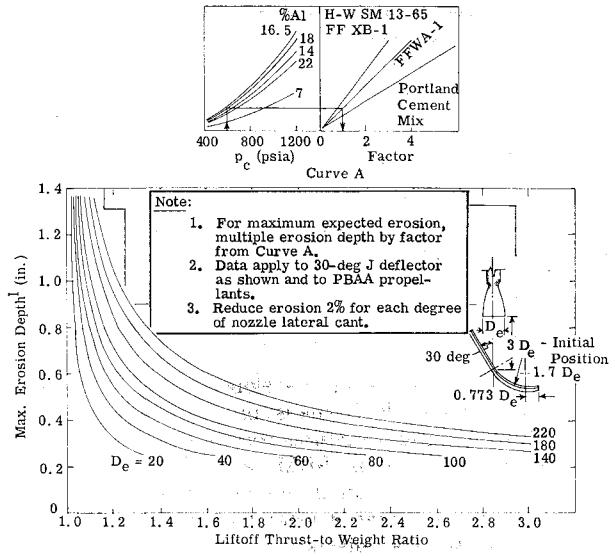

Fig. 15 Deflector erosion prediction nomograph.

Two classes of materials were considered: epoxies and silicones. The epoxies char on the surface and are good ablators. The char has good emittance characteristics and is porous, thus permitting a certain amount of surface cooling by transpiration. Silicones do not char unless the organic portion contains phenyl groups.

A large number of off-the-shelf thermal protective coatings were evaluated§ and ranked according to volume loss during simulated lift-off. Dynatherm E-300 performed best of the three top contenders on this basis, followed by Dow Corning Q90-006 and Martyte. Dynatherm E-300 and Martyte were more easily applied than Dow Corning Q90-006. Martyte is manufactured and sold by Presstite Division of Interchemical Corporation. Dynatherm E-300 and Martyte are ceramic impregnated expoxies, and Dow Corning Q90-006 is a silicone. Dynatherm E-300 features an asbestos fiber filler

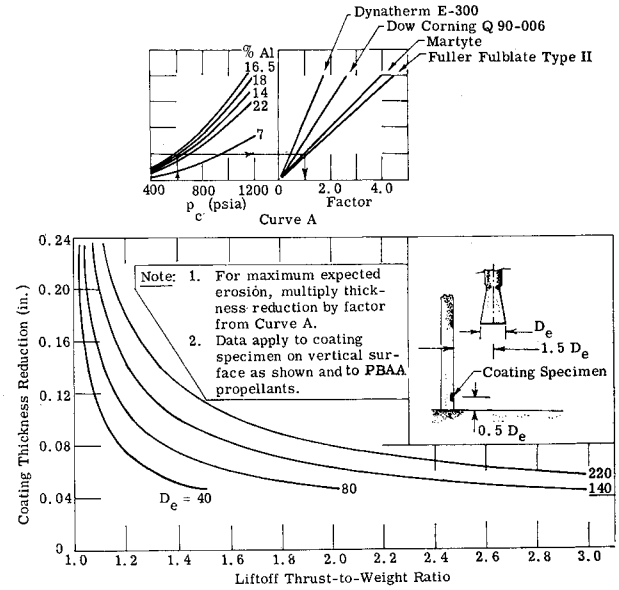

Fig. 16 Thermal protective coating erosion prediction nomograph.

§ Other coatings evaluated (not in the order of relative performance) were: Dow Corning Q20-103, Q30-121, and Q93-019; Fuller Fulblate 878 Types I and II; Fuller 190J-4 and Korblate II-190:L; General Electric RTV 511 and RTV 757 (foamed); and Raytheon RPR 2138, RPR 2141, and RPR 2156.

and glassy ceramic filler that softens and retains some of the char for future launches. It has additional transpiration formulated in the coating in the form of subliming inorganic oxides. Dow Corning Q90-006 contains iron oxide, which offers additional cooling since it is a good emitter of infrared radiation. The specific gravities of Dynatherm E-300, Dow Corning Q90-006, and Martyte are 1.2, 1.48, and 1.5, respectively. The nomograph in Fig. 16 allows prediction of exhaust effects on various preferred coatings for umbilical towers or other supporting equipment in the near-parallel flow regime.

Conclusions

Mathematical relationships developed for the prediction of effects of aluminized SRM exhaust products on deflectors and associated launch pad structures correlated with scale-model test results as well as 120-in. SRM data. Mechanical erosion is increased by the addition of aluminum to SRM grains, but the increment is an order of magnitude less than the erosion resulting from thermal effects. The addition of aluminum increases chamber temperature, and it is this additional heat, conducted more efficiently, that creates the greatest additional erosive action. The high heat fluxes coupled with the longer dwell times at the lower lift-off accelerations (high total heat of exposure) provide the most damaging environment.

A deflector radius of curvature equivalent to 1.7 D_e gives satisfactory exhaust plume deflection with predictable and nonexcessive deflector erosion. Curvature criterion and the required distance between the exit plane of the motor nozzle and deflector are governed more by vehicle constraints than by facility considerations (providing nozzle-exit-to-deflector distance is set greater than the length of the first supersonic shock diamond). Curvature and standoff criteria instrumentally affect vehicle base pressure and temperatures. In general, when umbilical towers and other launch pad structures remain farther than $1\frac{1}{2}$ D_e from the centerline of SRM's during launch and when nozzles are not canted toward the structure, heat protection is not required except in very localized areas.

The results of the SPREE program have enabled the launch facility designer to better cope with the exhaust environments associated with the launch of vehicles using large aluminized solid boosters.

References

[1] Schaafsma, W., "Special environmental measurements, DTP 1205-2," United Technology Corp., ER-UTC 63-174 (November 11, 1963).

[2] Hamilton, D. C. and Morgan, W. R., "Radiant-interchange configuration factors," NACA TN2836 (December 1952).

[3] Lays, E., Zaehringer, A., Chase, A., Mueller, G., and Farrington, W., "Solid propellant rocket exhaust effects (SPREE) and methods of attenuation," Martin Co., Denver, Colo., Phase II Final Report, Martin-CR-64-87 (Vol. 1) (December 1964).